

# Combined photoacoustic and ultrasound biomicroscopy

Tyler Harrison\*, Janaka C. Ranasinghesagara\*, Huihong Lu, Kory Mathewson, Andrew Walsh and Roger J. Zemp<sup>1</sup>

*Department of Electrical and Computer Engineering, University of Alberta, 9107 116 Street, Edmonton, AB T6G 2V4, CANADA*

<sup>1</sup>*zemp@ece.ualberta.ca*

**Abstract:** We report on the development of an imaging system capable of combined ultrasound and photoacoustic imaging based on a fast-scanning single-element 25-MHz ultrasound transducer and a unique light-delivery system. The system is capable of 20 ultrasound frames per second and slower photoacoustic frame rates limited by laser pulse-repetition rates. Laser and ultrasound pulses are interlaced for co-registration of photoacoustic and ultrasound images. In vivo imaging of a human finger permits ultrasonic visualization of vessel structures and speckle changes indicative of blood flow, while overlaid photoacoustic images highlight some small vessels that are not clear from the ultrasound scan. Photoacoustic images provide optical absorption contrast co-registered in the structural and blood-flow context of ultrasound with high-spatial resolution and may prove important for clinical diagnostics and basic science of the microvasculature.

©2009 Optical Society of America

**OCIS codes:** (170.5120) Photoacoustic imaging; (170.7170) Ultrasound, (170.3880) Medical and biological imaging, (170.5810) Scanning microscopy.

---

## References and links

1. M. Xu, and L. Wang, "Photoacoustic imaging in biomedicine," *Rev. Sci. Instrum.* **77**(4), 041101 (2006), doi:10.1063/1.2195024.
2. K. Maslov, H. F. Zhang, and L. V. Wang, "Effects of wavelength-dependent fluence attenuation on the noninvasive photoacoustic imaging of hemoglobin oxygen saturation in subcutaneous vasculature in vivo," *Inverse Probl.* **23**(6), S113–S122 (2007).
3. L. Li, H. F. Zhang, R. Zemp, K. Maslov, and L. V. Wang, "Simultaneous imaging of a lacZ-marked tumor and microvasculature morphology in vivo by dual-wavelength photoacoustic microscopy," *J. Innov. Opt. Health Sci.* **1**(02), 207–215 (2008).
4. E. Zhang, J. Laufer, and P. Beard, "Backward-mode multiwavelength photoacoustic scanner using a planar Fabry-Perot polymer film ultrasound sensor for high-resolution three-dimensional imaging of biological tissues," *Appl. Opt.* **47**(4), 561–577 (2008).
5. J. J. Niederhauser, M. Jaeger, R. Lemor, P. Weber, and M. Frenz, "Combined ultrasound and optoacoustic system for real-time high-contrast vascular imaging in vivo," *IEEE Trans. Med. Imaging* **24**(4), 436–440 (2005).
6. H. F. Zhang, K. Maslov, G. Stoica, and L. V. Wang, "Functional photoacoustic microscopy for high-resolution and noninvasive in vivo imaging," *Nat. Biotechnol.* **24**(7), 848–851 (2006).
7. R. J. Zemp, L. Song, R. Bitton, K. K. Shung, and L. V. Wang, "Realtime photoacoustic microscopy in vivo with a 30-MHz ultrasound array transducer," *Opt. Express* **16**(11), 7915–7928 (2008).
8. F. S. Foster, M. Y. Zhang, Y. Q. Zhou, G. Liu, J. Mehi, E. Cherin, K. A. Harasiewicz, B. G. Starkoski, L. Zan, D. A. Knapik, and S. L. Adamson, "A new ultrasound instrument for in vivo microimaging of mice," *Ultrasound Med. Biol.* **28**(9), 1165–1172 (2002).
9. L. V. Wang, "Prospects of photoacoustic tomography," *Med. Phys.* **35**(12), 5758–5767 (2008).
10. S. Hu, K. Maslov, V. Tsytarev, and L. V. Wang, "Functional transcranial brain imaging by optical-resolution photoacoustic microscopy," *J. Biomed. Opt.* **14**(4), 040503 (2009), doi:10.1117/1.3194136.

---

## 1. Introduction

Photoacoustic (PA) imaging provides optical absorption contrast with high depth-to-resolution ratios compared to other transport- and diffusion-regime optical imaging technologies [1]. It

has attracted considerable attention in the recent literature due to its capacity for functional [2] and molecular imaging [3], and for imaging microvascular networks [4].

We have developed a hybrid photoacoustic (PA) and ultrasound (US) imaging system to provide ultrasonic B-mode images as a structural context for optical-contrast photoacoustic B-scans. While some groups have already combined ultrasound and photoacoustic imaging at diagnostic frequencies (2-15MHz) [5]; to our knowledge this has not been done at high ultrasound frequencies (>20MHz) for real-time scanning rates. High-frequency photoacoustic microscopy (PAM) has provided outstanding images of microvascular structures to depths of 2-3 mm in vivo [6]. Our hybrid imaging system operates at 25-MHz and offers real-time ultrasound imaging capabilities at a resolution and depth-scale comparable with PAM parameters. Additionally, the ultrasound and laser pulses are interlaced in our system, providing natural co-registration of the two complementary contrasts. We believe that the combined ultrasound and photoacoustic biomicroscopy system provides significant diagnostic value over either standalone modality. Moreover, the addition of micro-ultrasound to PAM may prove important considering the recent proliferation of articles utilizing high-frequency ultrasound for pre-clinical studies.

While real-time photoacoustic imaging has been developed using a high-frequency array transducer [7], high-frequency arrays are only now coming on the market and can be cost-prohibitive. Moreover, real-time photoacoustic systems developed thus far lack ultrasound structural context. We believe that a viable alternative to these systems may be based on fast-scanning single element transducers, since such systems have proved to be a workhorse in many pre-clinical ultrasound imaging studies [8]. Unfortunately to use fast-scanning systems for real-time photoacoustic imaging requires high-repetition-rate lasers which are also cost-prohibitive. Our approach is to develop a fast-scanning single-element transducer system capable of high-frame-rate ultrasound imaging coupled with a slower-scanning photoacoustic mode (with interlaced ultrasound and laser pulses), frame-rate limited by the pulse-repetition-rate of the laser. We anticipate that B-mode ultrasound may be used for localizing a region of interest then the photoacoustic mode may be invoked to retrieve the optical contrast information in the desired location. While our future plan is to incorporate multi-wavelength photoacoustic imaging, the present study uses only a single optical wavelength at 532 nm. Our study shows that speckle-changes in ultrasound B-scans representing blood flow correlate with photoacoustic signatures – and that photoacoustic and ultrasound images each offer information that the sister modality cannot alone provide.

## 2. Method

### 2.1 Light delivery probe

We used a 532 nm pulsed laser (Ultra UL 421111, Big Sky Technologies, Bozeman, MT, USA) with a maximum pulse repetition rate of 20 Hz and pulse duration of 10 ns for this study. At the focus, the optical fluence was estimated as  $\sim 20$  mJ/cm<sup>2</sup>.

As shown in Fig. 1, we developed a light delivery probe based on dark field illumination. A 25-MHz ultrasound transducer with a 12.7-mm focal length and 6-mm active aperture (V324-SM, Panametrics, Waltham, MA, USA) is mounted within the lower part of the probe. A down-looking right angle prism mounted above the acrylic probe ( $n = 1.46$ ), which diverts the incident laser beam towards a 45° reflective cone to spread the light horizontally. The 45° polished surface of the probe reflects the horizontal light downward along the probe. Another polished face, machined at an angle smaller than the acrylic-water critical angle deflects light confocally around the transducer focal axis. Light is focused at  $\sim 10.5$ mm below the bottom of this probe. During setup, the ultrasound transducer position is adjusted vertically to match its focus point with the laser focus by maximizing the photoacoustic signal from the carbon fiber.

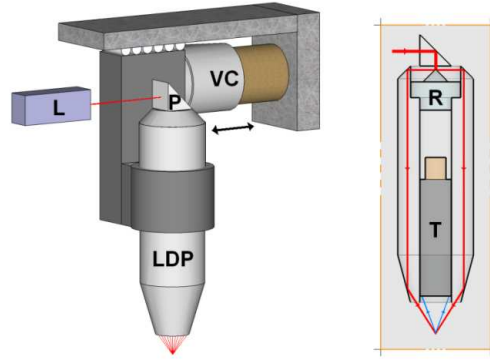


Fig. 1. Voice coil (VC) US/PA scanning system and cross section of Light Delivery Probe (LDP). Incident light from laser (L) is diverted towards the reflective cone (R) by the prism (P). Ultrasound transducer (T) is mounted inside the LDP.

## 2.2 Fast scanning system

The combined ultrasound transducer and light probe is mounted on a voice-coil stage. This stage is driven by a programmed motor controller to achieve up to 10-Hz oscillations over ~9mm, providing up to 20 imaging frames per second (higher rates are possible for shorter scan ranges). At present, our system provides three imaging modes: ultrasound mode, photoacoustic mode and interlaced ultrasound-photoacoustic mode. A system block diagram may be seen in Fig. 2.

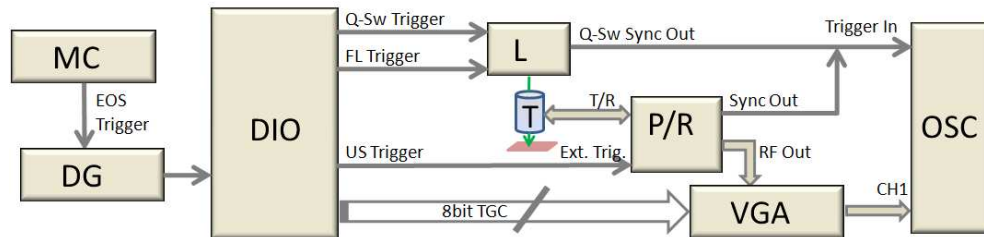


Fig. 2. Combined ultrasound-photoacoustic system block diagram. MC: Motor Controller; DG: Delay Generator; DIO: Digital Input Output card; L: Laser; T: Ultrasound Transducer; P/R: Ultrasound Pulsar/Receiver; VGA: Variable Gain Amplifier; OSC: Oscilloscope; Q-Sw: Q-Switch; FL: Flashlamp; EOS: End of Scan.

In the ultrasonic scanning mode, the motor controller (Elmo Harmonica HAR 5/60, Elmo Motion Control Inc., Nashua, NH, USA) drives the voice coil stage (VCS-10-023-BS-01, 1.0" travel, 2.3lbs continuous force, 6.9 lbs peak force, purchased from H2W technologies, Inc., Valencia, CA, USA) to oscillate at a fixed and desired scanning rate. A digital output bit from the motor controller is set to high for a short duration at the end of each scan trajectory. This end-of-scan trigger is used to mark the beginning of each image frame. This output event triggers a sequence of A-scan line trigger pulses which are generated by a digital input-output (DIO) card (NI PCI-6542, National Instruments Inc., Austin, TX, USA) and are sent to the ultrasound pulser-receiver (5703PR, Panametrics, Waltham, MA, USA). The ultrasound pulser-receiver is capable of a repetition rate up to 10 kHz, with excitation energy up to 16  $\mu$ J. The pre-amplifier built into the pulser-receiver provides gain of up to 39dB.

In the photoacoustic mode, the frame-rate is limited by the 20-Hz pulse repetition rate of the laser. Just as in the ultrasound mode, the end-of-scan causes the DIO card to generate a trigger sequence, this time for the laser flash-lamp trigger. However, there was an unacceptable jitter of multiple microseconds between the laser flash lamp trigger and the lasing output, so we also generate a pulse sequence for the laser's Q-switch trigger to reduce jitter to zero.

The variable-gain amplifier (VGA) is analog-voltage controlled via an 8-bit DAC (HI3338, Intersil, Milpitas, CA, USA) controlled by the DIO card. The particular VGA used (AD603ARZ evaluation board, Analog Devices, Norwood, MA, USA) is capable of an amplification range of 40 dB (−10dB to 30dB in the configuration used), with a response rate of 80 dB/μs. The time-gain compensation for photoacoustic modes is a constant gain of some small attenuation until about 7.5 μs to minimize unwanted signals (the focus is at 8.45 μs), then a ramp up to maximum gain at 11 μs. For ultrasound, a similar scheme is used, save that the ramp begins at 11 μs (the focus is at 16.9 μs) and achieves full gain at 24.6 μs, followed by a drop of about 6 dB at 31 μs, and a further drop to the original level at 34 μs.

### 2.3 Data acquisition

Data is currently acquired using an oscilloscope (DPO 7054, Tektronix, Beaverton, OR, USA), using a sampling rate of 500 MHz. Signal inputs are terminated at 50 Ω for impedance matching to the VGA. Acquisition triggers are provided by the sync-out outputs of the ultrasound pulser-receiver and the laser. Future improvements to the system will have data acquisition via a PCI card, allowing the entire system to be controlled by a single computer. For interlaced images, the horizontal delay of the oscilloscope is set to 6 μs and the length of the acquisition window is set to 20 μs. This allows us to capture total of 8.5 mm depth of a sample in both modes.

### 2.4 US-PA data mapping

Interlaced images are separated and plotted as standard B-mode ultrasound and photoacoustic images. To combine images, a simple program was written to co-register the images. The photoacoustic images were thresholded and superimposed on the ultrasound B-scans in an orange colormap.

## 3. Results

### 3.1 Resolution studies

A single 7.5-μm carbon fiber (Sigrafil C25 T060 EPY, SGL Group, Wisbaden, Germany) was imaged at different depths by using our system. The focal lateral resolution of the ultrasound mode was measured at  $140 \pm 10 \mu\text{m}$ , with accompanying axial resolution of  $<40\mu\text{m}$ . Lateral resolution of the photoacoustic mode was slightly worse at  $180 \pm 10 \mu\text{m}$  due to one-way, rather than 2-way focusing. Both were measured at the focus by taking the maxima along the appropriate direction, normalizing to the absolute maximum, plotting on a decibel scale, and finding the full-width half-maximum at the −6dB point. Images of the fiber at the focus are shown in Fig. 3a and 3b using US and PA modalities respectively.

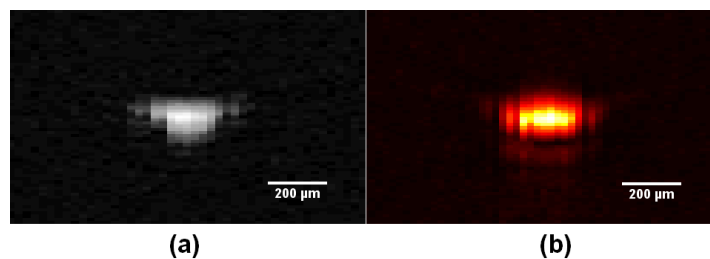


Fig. 3. Images of a carbon fiber at the focal position: (a) US (Log Scale); (b) PA.

### 3.2 In vivo imaging

To capture *in vivo* images, we imaged the underside tip of the ring finger of an adult subject's right hand, immersed in a water bath.

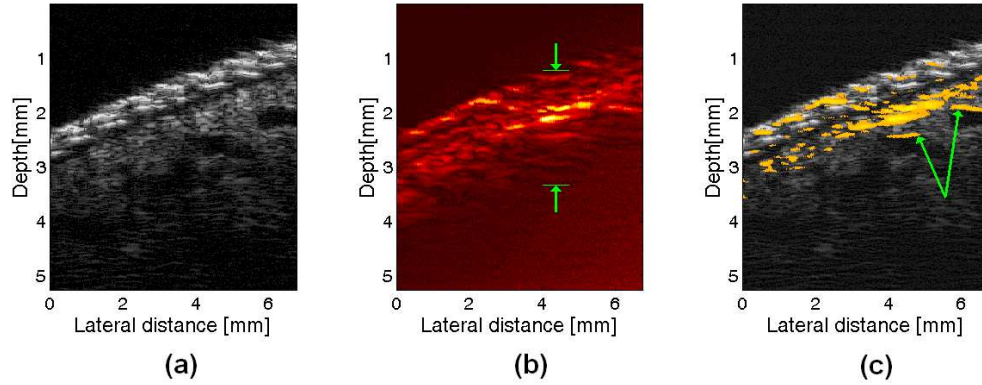


Fig. 4. US and PA images of human finger (a) US image; (b) PA image, arrows indicate effective photoacoustic imaging depth; (c) Combined image, arrows indicate where large vessels are seen only in part in PA data

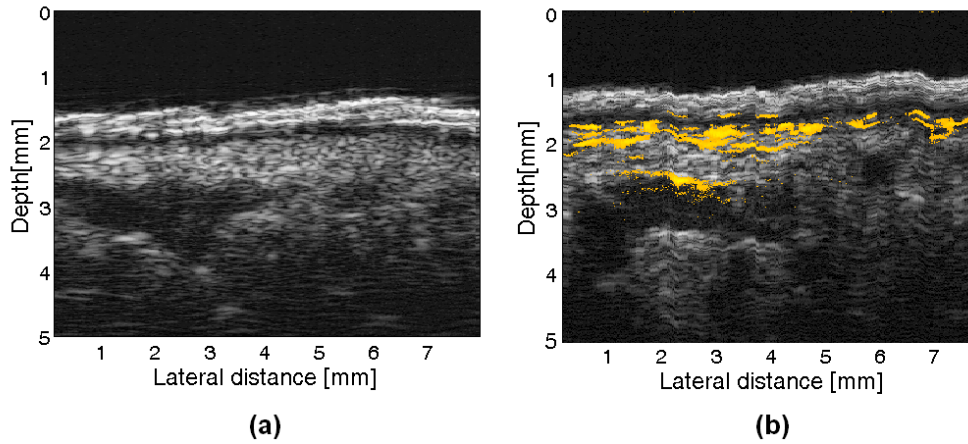


Fig. 5. Similar structures in movie frame ((a), [Media 1](#)) and a combined image (b)

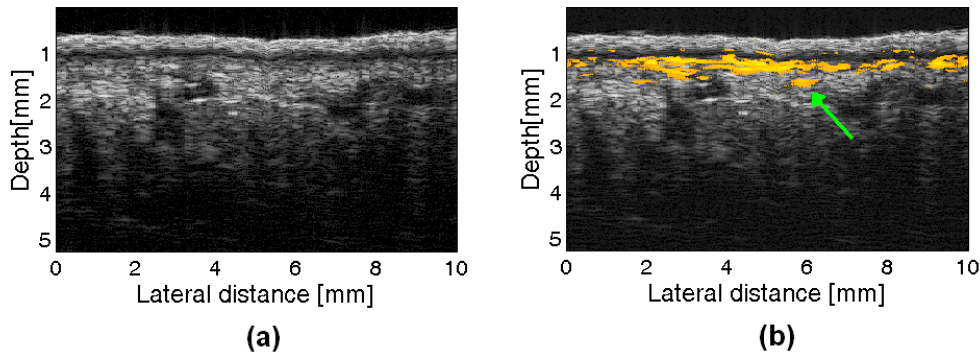


Fig. 6. Example of seeing vessel with PA (Green Arrow in (b)) that is not visible in US in (a)

Figure 4 shows the combined ultrasound-photoacoustic mode. The interleaved scans are separated to form individual images of ultrasound data (Fig. 4a), and photoacoustic data (Fig. 4b), then combined to form a composite image (Fig. 4c). Figure 5 provides a sample of the intended use of the system. First, an interesting structure may be located using the ultrasound-

only mode (Fig. 5a, [Media 1](#)), then the combined imaging mode may be used to form a more detailed image. In ([Media 1](#)), it is possible to see speckle changes, indicating blood flow, suggesting that this system may be suitable for color Doppler applications.

Figure 6 shows how the two imaging modalities can be used in a complimentary fashion. Figure 6a shows the ultrasound-only data, and Fig. 6b shows the combined image. In Fig. 6b, the photoacoustic image shows vascular structures not clearly present in the ultrasound-only image, an example of which is annotated by a green arrow.

#### 4. Discussion

The synergy of combining ultrasound and photoacoustic biomicroscopy is evident from viewing Fig. 4 to 6. ([Media 1](#)), acquired using the fast-scanning ultrasound mode, shows subcutaneous vessel structures and visible speckle changes within the vessel corresponding to blood flow. Photoacoustic imaging shows very fine vessel structures not evident from the ultrasound scan. Figure 6 shows a fairly prominent vessel that is clear from the photoacoustic scan but not the ultrasound scan. Conversely, ultrasound shows some large vessel structures that are too deep to be seen by photoacoustic imaging. Vessels on the right side of Fig. 4c are clearly seen in the ultrasound scan – and they have a corresponding photoacoustic signature, however, this signal is only seen at the top of the vessel. The principle reason for this is that the optical penetration depth of green light in whole blood is <50 microns.

From Fig. 4b, we gauge the photoacoustic penetration depth as roughly 2 mm. Improved penetration depth may be expected at longer optical wavelengths where the reduced scattering coefficient is less, and where penetration through blood is more. The present system uses 532 nm light due to laser availability. Penetration depth is limited by the attenuation of light and ultrasound, and by the depth of field of the single element transducer (~2mm).

Future work will incorporate a tunable laser system that operates at a higher pulse-repetition rate, thus enabling multiwavelength studies and faster imaging rates respectively. These and other future improvements, including realtime display, high-frequency arrays for dynamic focusing, and 3-D scanning should prove highly valuable for a number of pre-clinical & clinical studies concerned with microvascular morphology and function within a number of pathologies.

#### 5. Summary and conclusions

To our knowledge this is the first work that combines ultrasound and photoacoustic imaging at high frequencies (>20MHz) and fast imaging rates. By combining fast-scanning high-resolution ultrasound with photoacoustic microscopy we are able to see photoacoustic signatures in context of the surrounding tissue structures. Blood flow can be visualized in the B-scan movie, and overlaid photoacoustic images provide optical contrast information to the ultrasound backscatter information provided by pure ultrasound. Multiwavelength studies may open up doors to measure blood oxygen saturation and flow, which could pave the way to quantitative oxygen consumption measurements [9,10].

#### Acknowledgments

We are grateful to Dr. Robert Fedosejevs for sharing his Nd:YAG laser. This research was sponsored by the Canadian Cancer Society (NCIC TFF 019237 and 019249), the Natural Sciences & Engineering Research Council of Canada (NSERC 355544-08) and the Canada Foundation for Innovation. We also acknowledge NSERC & iCORE student scholarships.

\* Authors contributed equally.